One-shot active learning for vessel segmentation

Daniele Falcetta[1][0009−0009−7199−5424], Hava Chaptoukaev[1][0009−0000−0859−4059], Francesco Galati[1][0000−0001−6317−6298], and Maria A. Zuluaga[1,2][0000−0002−1147−766X]

[1] EURECOM, Biot, France
[2] School of Biomedical Engineering & Imaging Sciences, King's College London, UK
{daniele.falcetta,maria.zuluaga}@eurecom.fr

Abstract. Vessel segmentation is crucial for analyzing brain vasculature and understanding cerebral functions and disease mechanisms. Current deep-learning models for segmenting blood vessels within brain images are supervised and depend on extensive labeled data, which requires expert annotation and is both time-consuming and resource-intensive. To address these challenges, we propose Vessel-Dictionary Selection Net (V-DiSNet), a one-shot active learning (OSAL) framework specifically designed for vessels that can be used to select a small, representative set of informative and diverse samples for expert annotation and training, given an unlabeled dataset – in a single iteration. The selection process involves sampling from a latent space designed by leveraging the recurrent properties of brain vessel patterns. Specifically, we combine dictionary learning with k-means clustering to learn a latent representation integrating fundamental basis elements representing recurrent vessel features such as shape, connectivity, and structures. We experimentally demonstrate the effectiveness of our method on three publicly available 3D Magnetic Resonance Angiography datasets, showing that V-DisNet consistently outperforms random sampling and other state-of-the-art OSAL methods in terms of standard vessel segmentation metrics. Our code is available at github.com/i-vesseg/V-DiSNet.

Keywords: One-Shot Active Learning · Vessel Segmentation · Sparse Latent Representation

1   Introduction

Vessel segmentation is a crucial step in analyzing the brain vasculature and building a comprehensive vascular tree, which is fundamental for understanding brain function and the mechanisms underlying neurological disorders [4]. Recent state-of-the-art methods for brain vessel segmentation [2,6,9,19,22,27] build on deep learning (DL) architectures capable of capturing complex spatial relationships in volumetric brain scans, leading to highly accurate vessel delineations. Nevertheless, these models primarily rely on fully labeled datasets. Obtaining expert-level annotations is resource-intensive and time-consuming, particularly for intricate vascular structures [18].

Related Work. Several approaches have been proposed to alleviate the burden of exhaustive labeling. For instance, transfer learning [14,24], weakly supervised methods [3], and active learning (AL) strategies [10,16,21] aim to reduce the manual annotation effort while preserving segmentation accuracy. In particular, AL has received significant attention in medical imaging [1,25]. It reduces manual efforts by iteratively identifying the most informative unlabeled samples for expert annotation. Despite their success, classical AL frameworks typically involve several cycles of model re-training and querying an external oracle, demanding continuous availability of human annotators and incurring high computational costs [10]. This iterative overhead limits AL's practicality in settings where clinical resources and time may be constrained [26]. One-shot Active Learning (OSAL) addresses this limitation and enables the selection of a minimal set of informative samples in a single iteration. Unlike iterative AL, which re-trains models after each labeling round, OSAL automatically identifies the most informative samples to be annotated in a single pass, thus removing the need for repeated updates and human involvement. Existing OSAL frameworks rely on self-supervised learning [10], variational autoencoder [28] and contrastive learning with data augmentation [12,13] to select a minimal set of samples to be labeled, that maximize segmentation performances. However, these models do not provide an explicit mechanism to ensure that the selected set is meaningful. In brain vessel segmentation for example, samples selected using OSAL may not fully reflect the underlying anatomy of the brain, as they fail to take into account the recurring tree-like structures of brain vessels. Additionally, the lack of interpretability of their selection processes, which do not provide insights into why some data points are prioritized over others, makes it hard to ensure that the identified samples representative of the full data. This is particularly concerning since non-representative samples may lead to a lack of generalization abilities, ultimately leading to suboptimal performance on new unseen data.

Contributions. To address these limitations, we propose Vessel-Dictionary Selection Net (**V-DiSNet**), a novel OSAL framework tailored to the complex, tree-like geometry of brain vessels. Our model combines dictionary learning with k-means clustering to explicitly capture and model the recurrent tubular structures, or *patterns*, of brain vessels, and identify a minimal set of groups that are representative of the full vascular tree. We use these learned groups to guide the construction of an interpretable and robust sparse latent representation of vascular patterns – that provides insights into the underlying brain anatomy. We then design a single-pass querying strategy that leverages the learned latent space to efficiently select a minimal yet representative and informative set of patches for external annotation, that can be used to train brain vessel segmentation models. To the best of our knowledge, V-DisNet is the first OSAL framework designed specifically to take advantage of the recurring nature of brain vessel patterns.
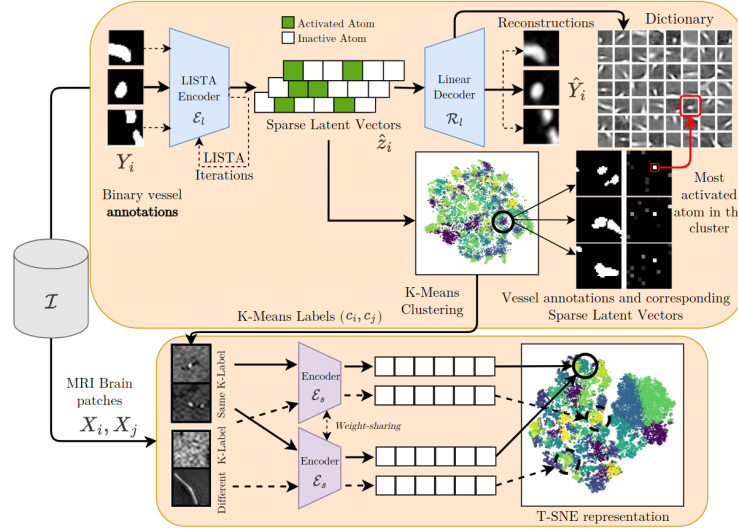
Fig. 1: Overview of the V-DiSNet framework: A one-shot active learning pipeline that leverages dictionary learning to capture intrinsic vessel patterns, constructs an informative latent space via a Siamese encoder, and applies diversity-based sampling to select a minimal yet representative set of vessel patches for efficient brain vessel segmentation.

2   Method

Under the assumption that a brain vessel tree results from a set of hierarchical tree-like recurring branching patterns [20,23], a vascular tree can be modeled as a linear combination of dictionary elements, such that $\mathbf{Y} = \mathcal{B}\mathbf{z}$, where $\mathcal{B}$ is an over-complete dictionary of image patches of tree-like branching patterns of vessels, and $\mathbf{z} \in \mathbb{R}^K$ is a sparse vector containing the representation coefficients of the vascular tree image $\mathbf{Y}$. As the dictionary is not directly observed, we aim to infer its elements, or *atoms*, from observed annotated data. We propose a novel framework to (1) learn a reduced dictionary that fully captures the range of recurring brain vessel patterns, (2) learn an informative latent representation of brain MRI patches using the previously extracted patterns, and (3) use the learned latent space to sample a minimal set of patches that offer maximum coverage of vessel patterns, to be manually annotated before training segmentation models given a new unlabeled dataset. Fig. 1 illustrates our proposed framework.

Identifying recurring vessel patterns We consider a labeled dataset $\mathcal{I}$. Given an image $\mathbf{I}$ and its associated label map $\mathbf{L}$, $(\mathbf{I}, \mathbf{L}) \in \mathcal{I}$, of size $H \times W \times S$, as in [3], for each slices $X_s \in \mathbf{I}$, and $Y_s \in \mathbf{L}$ we consider the partitions into P_s non-overlapping patches $\mathcal{X}_s = \{X_k\}_{k=1}^{P_s}$ and $\mathcal{Y}_s = \{Y_k\}_{k=1}^{P_s}$. We build a set of binary vessel annotated patches $\mathcal{Y}_\mathcal{I}$, such that $\mathcal{Y}_\mathbf{L} = \{\mathcal{Y}_s\}_{s=1}^S$ and $\mathcal{Y}_\mathcal{I} = \{\mathcal{Y}_\mathbf{L}\}_{\mathbf{L} \in \mathcal{I}}$.

The dictionary of recurring vessel patterns can then be obtained by solving:

$$\hat{\mathcal{B}}, \hat{\mathbf{Z}} = \min_{\mathcal{B}, \mathbf{Z}} \|\mathcal{Y}_{\mathcal{I}} - \mathcal{B}\mathbf{Z}\|_2^2, \tag{1}$$

subject to $\|\mathbf{Z}\|_1 < \lambda$. The columns of $\mathbf{Z}$ are formed by the representation coefficient vectors $\hat{z}_i$, and λ is a regularization parameter controlling the sparsity of the representation coefficient vectors. We use the learned iterative shrinkage thresholding algorithm (LISTA) [7] to solve the optimization problem in Eq. 1. Annotated patches $Y_i \in \mathcal{Y}_{\mathcal{I}}$ are first encoded through a linear encoder $\mathcal{E}_1$ into sparse latent vectors $\hat{z}_i$, where each element of a vector corresponds to an atom that can either be activated or idle (i.e., zero-valued). The representations $\hat{z}_i$ are then passed through a linear decoder $\mathcal{R}_1$ to ultimately obtain the reconstructed $\hat{\mathcal{Y}}_{\mathcal{I}} = \hat{\mathcal{B}}\hat{\mathbf{Z}}$, where the learned latent sparse vectors $\hat{\mathbf{Z}}$ capture the recurrent patterns of vessel trees. Ultimately, we aim to learn the smallest set of patterns that is representative of the recurrent patterns of vessel trees. We propose to apply k-means clustering on the sparse latent vectors $\hat{\mathbf{Z}}$ to group the elements, or *atoms*, of the obtained dictionary into clusters based on their sparse latent features. A cluster label c_i is assigned to each annotation Y_i and corresponding image patch X_i of the dataset, thus reducing the number of distinct vessel patterns to the number of distinct clusters c_i. Figure 1 illustrates some examples of activated atoms, highlighted in green, capturing essential vessel features such as shape, connectivity, and position within the patch.

Latent Space Generation for MRI patches We then use the structural information extracted from the obtained patterns to train an encoder to generate an informative latent space of brain patches. In this second stage, pairs of MRI brain patches X_i, X_j and their corresponding k-means labels c_i, c_j are fed into a Siamese encoder network $\mathcal{E}_s$, where weight-sharing is implemented between the encoders to ensure consistent representation learning. For patches with the same k-means label, $c_i = c_j$, $\mathcal{E}_s$ aims to produce similar latent vector representations. In contrast, for patches with different k-means labels $c_i \neq c_j$, the encoder seeks to differentiate their representations. This process ensures that patches with similar vessel patterns are closely represented in the embedding space, while those with different structures are more distinctly separated, thereby enriching the latent space discriminative power.

Diversity Sampling and Segmentation Lastly, we use our framework to identify a minimal subset of n brain patches for annotation by an external oracle, which will then be used to train a segmentation model. Given a new dataset of unlabeled images $\mathcal{I}^U = \{I_j\}_{j=1}^M \subset \mathbb{R}^{H \times W \times S}$, where I_j is the j-th image in the dataset, without any associated label map. For each slice X_s^U, we partition the image into P_s non-overlapping patches $\mathcal{X}_s^U = \{X_k^U\}_{k=1}^{P_s}$. These patches are fed into the previously trained $\mathcal{E}_s$ to generate their corresponding latent vectors $z_k^U \in \mathcal{Z}^U$. The different groups of patterns are then extracted using k-means to identify regions of varying density and different vessel patterns within the latent representation of the patches from the new dataset. We use a stratified version of the farthest point sampling (FPS) algorithm [15] to randomly select n patches from both densely and sparsely populated regions of the latent space,

thus maximizing coverage. As a result, this subset of n patches is diverse and representative of the underlying data distribution, leading to a final training set that includes a broad spectrum of the vessel patterns present in the unlabeled dataset. Finally, the selected patches are annotated by an external oracle to obtain a training set that can be used to enhance the robustness and performance of a subsequent segmentation model Φ.

3 Experiments and Results

Experimental Setup. We use the **IXI** dataset as $\mathcal{I}$ to learn vessel patterns and train an encoder for clustering structurally similar vessel patches. Specifically, 22 TOF-MRA volumes (median grid: $359 \times 481 \times 100$, voxel size: $0.47 \times 0.47 \times 0.80$ mm) were sampled from healthy subjects aged 20–86. Each includes brain masks (HD-Bet [11]) and expert-annotated vessel masks. We demonstrate our method on three public 3D-TOF MRA datasets ($\mathcal{I}^U$): **OASIS-3**, **SMILE-UHURA**, and **CAS**. *CAS* contains 100 volumes (median grid: $608 \times 640 \times 150$, voxel size: $1.00 \times 1.00 \times 1.00$ mm), split into 85 for training and 15 for testing. *OASIS-3* has 49 volumes (median dimension: $576 \times 768 \times 232$, voxel size: $0.60 \times 0.30 \times 0.30$ mm), of which 39 are used for training and 10 for testing. *SMILE-UHURA* includes 14 volumes (median dimension: $480 \times 640 \times 163$, voxel size: $0.30 \times 0.30 \times 0.30$ mm), split per challenge guidelines. All scans are resampled to the median spacing, skull-stripped, and standardized. Following [3] methodology, we extract 32×32 patches: 1,000 per subject (500 with vessels centered, 500 with vessels off-center), plus 500 non-vessel MRI patches from $\mathcal{I}^U$, totaling 1,500 patches per subject. Each patch is normalized by the overall dataset mean and standard deviation. At inference, overlapping patches (0.5 stride, 0.5 threshold) are used to address boundary uncertainties, with test patches normalized using training statistics.

Implementation Details. We use a dictionary learning model with LISTA [7] as a pretext reconstruction task to extract vessel pattern structures in a sparse latent space. We perform 3 LISTA iterations during training, using a final embedding dimension of 128, an MSE reconstruction loss, and hyper-parameters from [5]. Peak Signal-to-Noise Ratio (PSNR) is used to quantify reconstruction quality. For the MRI latent space construction, we use a Siamese network [17] with shared weights, trained for 200 epochs, with a LR of 5e−4 and early stopping. We adopt a contrastive loss [8], which imposes a margin between dissimilar pairs based on Euclidean distances in the latent space. We adopt the W-Net from [3] as our backbone architecture Φ. We train for 15k steps, with a batch size of 128 patches and early stopping. We use the Adam optimizer with a learning rate (LR) of 1e−4. We use the Dice and clDice metrics to assess segmentation quality of Φ. While Dice measures spatial overlap between predictions and ground truth, clDice further accounts for connectivity to preserve tubular structures like vessels, capturing both region accuracy and structural integrity. All experiments are implemented in PyTorch 1.19 on a single Nvidia-TITAN Xp GPU.

Table 1: Segmentation performance on 15 CAS dataset test patients at various labeling percentages. Eight experiments with distinct random seeds were run for each fraction and model to ensure robustness, with results averaged and standard deviations computed across test patients.

Labeled	(a) Dice Score (%)					(b) ClDice Score (%)				
(%)	V-DiSNet	R-W	RA	CA	AET	V-DiSNet	R-W	RA	CA	AET
0.1	**59.3±8.2**	50.4±5.3	57.6±5.1	55.1±4.8	56.3±4.9	**50.8±9.2**	41.9±6.6	49.3±5.8	47.5±6.7	48.4±.6.3
1	**71.9±2.4**	68.9±4.7	70.3±1.7	70.4±2.8	70.3±2.3	**68.5±3.9**	65.0±5.8	67.0±2.1	67.4±2.7	67.2±2.4
5	**77.4±1.4**	75.3±1.7	75.8±1.6	77.1±1.8	76.4±1.7	73.6±1.6	71.9±2.2	72.9±1.7	**74.0±1.7**	73.4±1.7
10	**79.8±0.8**	78.0±1.0	78.5±1.3	78.8±1.4	78.6±1.4	**765±0.5**	75.1±0.6	75.4±1.3	75.3±1.6	75.3±1.5
30	**81.5±0.7**	80.1±0.6	80.4±0.9	81.0±1.0	80.7±0.9	**77.9±1.1**	77.1±0.8	76.8±0.8	76.9±1.5	76.8±1.1
50	**82.0±0.6**	80.8±0.8	81.0±0.7	81.8±0.8	81.5±0.7	**78.0±0.9**	77.4±1.0	77.4±0.7	77.8±0.7	77.8±0.7
75	**82.0±0.7**	81.9±1.1	81.4±1.0	**82.0±0.7**	81.7±0.8	**78.3±0.7**	77.9±1.1	78.0±0.9	78.1±1.1	78.1±1.0

Segmentation Performances. We compare our model against random sampling (R-W) and three OSAL state-of-the-art methods, i.e., RA [28], CA [13], and AET [12], using 0.1–75% labeled data from the **CAS** dataset. To ensure the robustness of our findings, we conducted eight experiments for each fraction and model, each with a different random seed. The performances (Tab. 1) highlight how V-DiSNet consistently outperforms competitors across all fractions, particularly at lower sampling rates (0.1–10%). Crucially, with only 30% labeled data, V-DiSNet nearly matches the fully annotated dataset. This highlights the effectiveness of our sampling strategy in selecting informative patches and leveraging a robust latent space to enhance vessel segmentation. Additionally, we evaluate the robustness of V-DiSNet on **OASIS-3** and **SMILE-UHURA** (Fig. 2), using different labeled percentages and comparing against random sampling. Our method consistently outperforms the baseline, especially at lower annotation levels, and achieves, as before, near full-data performance with roughly 30% labels.

Identifying Informative Vessel Patches. To assess our dictionary learning model's ability to capture a rich and interpretable latent space, we apply it to a vessel patch reconstruction pretext task. As shown in Fig. 3, each input patch is encoded into a sparse latent vector whose active dictionary atoms reconstruct vessel features with high fidelity (PSNR of 28.89 ± 3.61 and $91 \pm 3\%$ sparsity). As intended, patches share dominant atoms within each cluster – reflecting consistent structural patterns across vessel patches. Fig. 3 also demonstrates how selectively deactivating or overactivating specific atoms alters vessel shape, size, or orientation. This suggests that the learned latent representations are meaningful, as specific atoms provide insights into specific structures of vessels – highlighting the interpretability of our method.

Clustering of Vessel Patches. To examine how well our model groups morphologically similar vessel patches, we applied the Elbow Method and found 50 clusters as the optimal value. Fig. 4 show cluster centroids and representative patches for a few selected clusters, revealing consistent structures (e.g., curvature, thickness). These clusters underline the model's ability to detect diverse
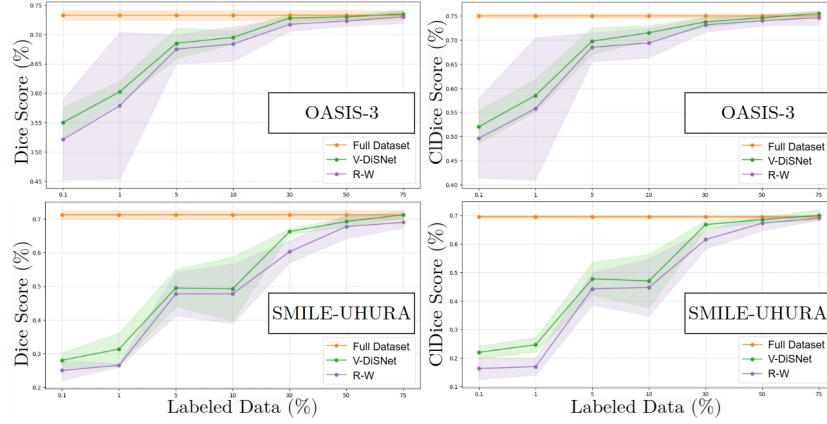
Fig. 2: Segmentation results on the OASIS-3 and SMILE-UHURA datasets, showing Dice scores (left) and ClDice scores (right) for different percentages of sample and annotated patches.

vessel anatomies and emphasize the need for a balanced sampling strategy that captures a variety of vessel patterns.

Ablation Study. We evaluated the roles of the *sampling technique* and the *patch size* in our framework. First, we compared our V-DiSNet stratified FPS sampling technique with stratified random sampling (R-C) and T-SNE-based FPS (T-FPS). As shown in Fig. 5 (left), V-DiSNet provides broader latent space coverage and stronger performance, especially under limited data conditions. Then, we examined the effect of the patch size by testing larger patches (Fig. 5, right) and found that smaller patches more effectively capture fine-grained vessel structures and yield higher Dice and clDice scores, offering a favorable solution in terms of accuracy and computational cost.

4   Conclusion

In this work, we introduced V-DiSNet, a novel OSAL framework tailored for brain vessel segmentation. By leveraging dictionary learning to construct a sparse latent space that captures the intrinsic recurring patterns of brain vessels, our method effectively identifies a minimal yet highly informative subset of patches for annotation. Experimental evaluations across three public 3D-TOF MRA datasets demonstrated that V-DiSNet consistently outperforms both random sampling and established one-shot active learning baselines, particularly under scenarios with limited labeled data. Notably, our approach nearly achieves the performance of fully supervised methods with only 30% of the labels, significantly reducing the annotation burden without compromising segmentation quality.

In addition, the dictionary atoms learned by V-DisNet also provide valuable and interpretable insights into vascular architecture and branching patterns,
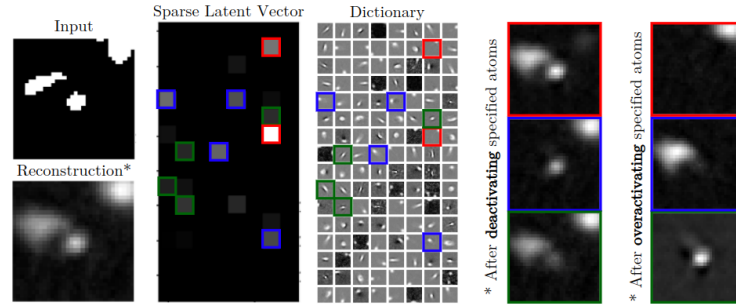
Fig. 3: Interpretability of V-DiSNet's sparse latent space. The input patch is encoded into a sparse representation using learned dictionary atoms. Deactivating or over activating specific atoms alters specific vessel components, highlighting their role in the reconstruction
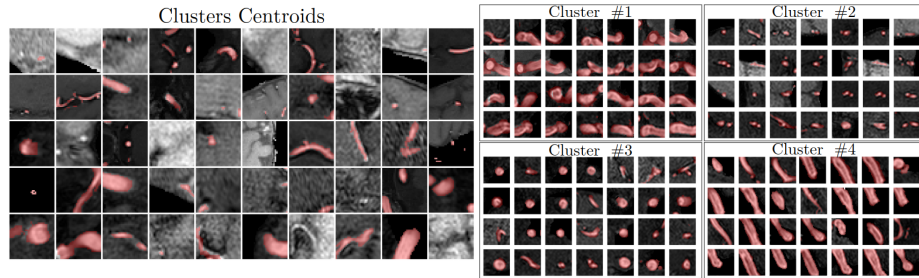

Fig. 4: Centroid images representing clusters of vessel patches extracted from 3D MRA brain image volumes (left); and examples of clusters of brain patches characterized by similar vessel features, such as shape, size, or position (right).

which can aid both clinical interpretation and model refinement. Overall, V-DisNet is an efficient, effective, and interpretable strategy for overcoming the challenges of limited annotated data in medical imaging. Future work will explore extending our framework to other vascular imaging modalities, integrating domain-specific knowledge to further enhance the vessel pattern representations, and investigating the transferability of learned dictionaries across different anatomical regions.
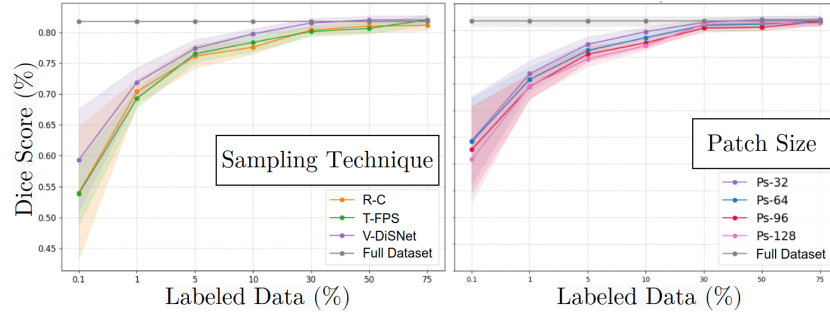
Fig. 5: Ablation study contrasting different *sampling strategies* in our learned latent space (left). Evaluation of the impact of the parameter *patch size* within our framework (right).

References

1. Budd, S., Robinson, E.C., Kainz, B.: A survey on active learning and human-in-the-loop deep learning for medical image analysis. Medical image analysis **71**, 102062 (2021)
2. Chen, Y., Fan, S., Chen, Y., Che, C., Cao, X., He, X., Song, X., Zhao, F.: Vessel segmentation from volumetric images: a multi-scale double-pathway network with class-balanced loss at the voxel level. Medical Physics **48**(7), 3804–3814 (2021)
3. Dang, V.N., Galati, F., Cortese, R., Di Giacomo, G., Marconetto, V., Mathur, P., Lekadir, K., Lorenzi, M., Prados, F., Zuluaga, M.A.: Vessel-CAPTCHA: An efficient learning framework for vessel annotation and segmentation. Medical Image Analysis **75**, 102263 (2022)
4. Deshpande, A., Jamilpour, N., Jiang, B., Michel, P., Eskandari, A., Kidwell, C., Wintermark, M., Laksari, K.: Automatic segmentation, feature extraction and comparison of healthy and stroke cerebral vasculature. NeuroImage: Clinical **30**, 102573 (2021)
5. Evtimova, K., LeCun, Y.: Sparse coding with multi-layer decoders using variance regularization. Transactions on Machine Learning Research (2022)
6. Fu, F., Wei, J., Zhang, M., et al.: Rapid vessel segmentation and reconstruction of head and neck angiograms using 3D convolutional neural network. Nature Communications **11**(1), 4829 (2020)
7. Gregor, K., LeCun, Y.: Learning fast approximations of sparse coding. In: Proceedings of the 27th International Conference on Machine Learning. pp. 399–406 (2010)
8. Hadsell, R., Chopra, S., LeCun, Y.: Dimensionality reduction by learning an invariant mapping. In: 2006 IEEE Computer Society Conference on Computer Vision and Pattern Recognition (CVPR'06). vol. 2, pp. 1735–1742 (2006)
9. Hilbert, A., Madai, V.I., Akay, E.M., Aydin, O.U., Behland, J., Sobesky, J., Galinovic, I., Khalil, A.A., Taha, A.A., Wuerfel, J., et al.: BRAVE-NET: fully automated arterial brain vessel segmentation in patients with cerebrovascular disease. Frontiers in Artificial Intelligence **3**, 552258 (2020)
10. Huang, S.J., Li, Y., Sun, Y., Tang, Y.P.: One-shot active learning based on lewis weight sampling for multiple deep models. arXiv preprint arXiv:2405.14121 (2024)

11. Isensee, F., Schell, M., Pflueger, I., Brugnara, G., Bonekamp, D., Neuberger, U., Wick, A., Schlemmer, H.P., Heiland, S., Wick, W., et al.: Automated brain extraction of multisequence MRI using artificial neural networks. Human Brain Mapping **40**(17), 4952–4964 (2019)
12. Jin, Q., Li, S., Du, X., Yuan, M., Wang, M., Song, Z.: Density-based one-shot active learning for image segmentation. Engineering Applications of Artificial Intelligence **126**, 106805 (2023)
13. Jin, Q., Yuan, M., Qiao, Q., Song, Z.: One-shot active learning for image segmentation via contrastive learning and diversity-based sampling. Knowledge-Based Systems **241**, 108278 (2022)
14. Keshavarzi, A., Angelini, E.: Few-Shot Airway-Tree Modeling Using Data-Driven Sparse Priors. In: 2024 IEEE International Symposium on Biomedical Imaging (ISBI). pp. 1–5 (2024)
15. Li, J., Zhou, J., Xiong, Y., Chen, X., Chakrabarti, C.: An adjustable farthest point sampling method for approximately-sorted point cloud data. In: IEEE workshop on signal processing systems (SiPS). pp. 1–6 (2022)
16. Li, W., Zhang, M., Chen, D.: Fundus retinal blood vessel segmentation based on active learning. In: 2020 International conference on computer information and big data applications (CIBDA). pp. 264–268 (2020)
17. Melekhov, I., Kannala, J., Rahtu, E.: Siamese network features for image matching. In: 2016 23rd international conference on pattern recognition (ICPR). pp. 378–383 (2016)
18. Moccia, S., De Momi, E., El Hadji, S., Mattos, L.S.: Blood vessel segmentation algorithms — review of methods, datasets and evaluation metrics. Computer Methods and Programs in Biomedicine (2018)
19. Ni, J., Wu, J., Wang, H., Tong, J., Chen, Z., Wong, K.K., Abbott, D.: Global channel attention networks for intracranial vessel segmentation. Computers in Biology and Medicine **118**, 103639 (2020)
20. Red-Horse, K., Siekmann, A.F.: Veins and arteries build hierarchical branching patterns differently: Bottom-up versus top-down. Bioessays **41**(3), 1800198 (2019)
21. Saeed, S.U., Ramalhinho, J., Pinnock, M., Shen, Z., Fu, Y., Montaña-Brown, N., Bonmati, E., Barratt, D.C., Pereira, S.P., Davidson, B., et al.: Active learning using adaptable task-based prioritisation. Medical Image Analysis **95**, 103181 (2024)
22. Shi, P., Guo, X., Yang, Y., Ye, C., Ma, T.: Nextou: Efficient topology-aware U-Net for medical image segmentation. arXiv preprint arXiv:2305.15911 (2023)
23. Tekin, E., Hunt, D., Newberry, M.G., Savage, V.M.: Do vascular networks branch optimally or randomly across spatial scales? PLoS computational biology **12**(11), e1005223 (2016)
24. Tetteh, G., Efremov, V., Forkert, N.D., Schneider, M., Kirschke, J., Weber, B., Zimmer, C., Piraud, M., Menze, B.H.: DeepVesselNet: Vessel segmentation, centerline prediction, and bifurcation detection in 3D angiographic volumes. Frontiers in Neuroscience **14**, 592352 (2020)
25. Wang, H., Jin, Q., Li, S., Liu, S., Wang, M., Song, Z.: A comprehensive survey on deep active learning and its applications in medical image analysis. arXiv preprint arXiv:2310.14230 (2023)
26. Yang, Y., Loog, M.: Single shot active learning using pseudo annotators. Pattern Recognition **89**, 22–31 (2019)
27. Zhang, H., Xia, L., Song, R., Yang, J., Hao, H., Liu, J., Zhao, Y.: Cerebrovascular segmentation in MRA via reverse edge attention network. In: Medical Image Computing and Computer Assisted Intervention–MICCAI. pp. 66–75 (2020)

28. Zheng, H., Yang, L., Chen, J., Han, J., Zhang, Y., Liang, P., Zhao, Z., Wang, C., Chen, D.Z.: Biomedical image segmentation via representative annotation. Proceedings of the AAAI Conference on Artificial Intelligence **33**(01), 5901–5908 (2019)